

# Synthesis and mechanical and thermal properties of multiblock terpoly(ester-ether-amide) thermoplastic elastomers with variable mole ratio of ether and amide block

Beata Schmidt, Joanna Rokicka

Department of Chemical Organic Technology and Polymeric Materials, Faculty of Chemical Technology and Engineering, West Pomeranian University of Technology, Szczecin; Pułaskiego 10, 70-322 Szczecin, Poland,

\*Corresponding author: e-mail: Beata.Schmidt@zut.edu.pl

A series of the terpolymers of poly[(trimethylene terephthalate)-block-(oxytetramethylene)-block-lauro lactam] with a variable molar ratio of ether and amide block and constant molecular weights of PA12 = 2000 g/mole and PTMO = 1000 g/mole have been obtained. The influence of changes of these molar ratios on the functional properties and the values of phase change temperatures of the products have been determined. The thermal properties and the phase separation of obtained systems were defined by DSC, DMTA and WAXS methods. The chemical structure of obtained materials was studied by FT-IR and <sup>13</sup>C NMR methods. The mechanical and elastic properties of these polymers were evaluated.

**Keywords:** poly(ester-b-ether-b-amide), multiblock elastomers, elastomers, phase structure.

## INTRODUCTION

Thanks to their excellent mechanical and physical properties thermoplastic elastomers (TPE) have found wide applications in many industrial branches as engineering materials. TPE combines the properties of vulcanized rubber and thermoplastics. These polymers are characterized by high elastic recovery, good flexibility at low temperatures like vulcanized rubbers, but they have great impact strength and may be processed simply like thermoplastics<sup>1-3</sup>.

The multiblock TPE macromolecule consists of flexible and rigid blocks with different physical and chemical properties. Flexible blocks are able to form a continuous matrix, most often it is a soft-elastic phase. As a result of aggregation, rigid blocks form a hard phase, usually dispersed. The characteristic feature of TPE is capable of microphase (nanophase) separation<sup>4-6</sup>. As a result of this phenomenon, two (or more) phases are distinguished, differing in the values of physical transformation temperatures. These temperatures determine the broad “plateau” of the modulus of elasticity. A matrix-domain structure is created<sup>2, 3, 6-8</sup>.

TPE properties are the result of combining the features of individual blocks. When designing multi-block systems, the type of blocks should be selected appropriately, paying attention to their chemical structure, chemical and physical properties as well as weight and molar ratios. Due to their properties polyamides (stiffness and excellent thermal and mechanical properties), polyesters (biocompatibility and biodegradability) and polyethers (relatively low price, increasing the elastic properties of the system) are often used as TPE blocks<sup>9-22</sup>.

The aim of the study was to obtain a series of thermoplastic elastomers by reaction of  $\alpha$ ,  $\omega$ -dicarboxyl(oligo laurinolactam) (PA12) with oligo(oxytetramethylene) diol (PTMO) and with dimethyl terephthalate and 1,3-propanediol (forming a block of poly(trimethylene terephthalate - during the synthesis) PTT). The effect of changing the molar ratio of ether to amide blocks on the properties of terpolymers obtained was investigated.

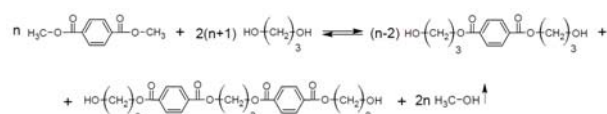
## EXPERIMENTAL

### Materials

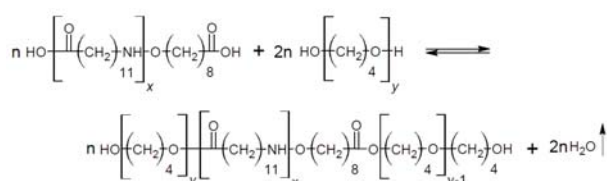
The following substrates were used: 1,3-propanediol (1,3-PDO; Sigma-Aldrich, USA), dimethyl terephthalate (DMT; Elana, Poland), poly(oxytetramethylene)diol with molecular weight 1000 g/mol (PTMO; Du Pont, USA), dodecano-12-lactam, sebacic acid – (Sigma-Aldrich, USA). The lactam and the dicarboxylic acid are the substrates prepared in our laboratory  $\alpha,\omega$ -dicarboxylic oligo(lauro lactam) (PA12) with the number average molecular weight 2000 g/mol<sup>16, 19</sup>, pentaerythritol (Brenntag, Poland), a titanate catalyst (TiO<sub>2</sub>/SiO<sub>2</sub>, Sachtleben Chemic GmbH, Germany), thermal stabilizers (Irganox 1010, Irgafos 126, Ciba Geigy, Switzerland).

### Synthesis of multiblock PTT-b-PTMO-b-PA12 polymers

The synthesis of PTT-b-PTMO-b-PA12 terpolymers consisted of the structural modification of PTT macromolecule. Some fragments derived from terephthalic acid have been replaced by a dicarboxylic oligoamide block and some derived from propylene glycol by a diol oligoether block. Synthesis of block terpolymers proceeded as a two-step process. The initial stage was the transesterification reaction of DMT with 1,3-PDO leading to the formation of polyester and the release of methanol (Equation 1) and the esterification (in a separate reactor) of PA12 with PTMO (by-product is water) in the presence of titanate catalyst (Equation 2). From



Equation 1. Transesterification reaction of DMT with 1,3-PDO



Equation 2. Esterification reaction of PA12 with PTMO

the respective amounts of methanol and water, it was concluded that the conversion in the transesterification reaction was 95% and the degree of esterification was 90% (degrees was expressed as the weight ratios of the released methanol or water to the respective stoichiometric amounts of these products). The second stage of the process comprises the proper condensation polymerization of mixed intermediates obtained in the first stage of synthesis.

## Methods

The limiting viscosity number  $[\eta]$  of the terpolymers in phenol-tetrachloroethylene mixture (60:40 vol/vol) was determined by an Ubbelohde viscometer II at 30 °C. Optical melting points  $T_m$  were determined using a Boetius microscope (HMK type Franz Kustner Nacht KG) at a heating rate of 2 °C/min. Hardness (H) measurements were performed on a Shore A and D apparatus (Zwick, type 3100) according to PN-80/C-04238. Swelling in the benzene and water ( $p_{H_2O}$ ,  $p_b$ ) was performed according to PN-66/C-08932. FT-IR analyses were carried out on a spectrometer Nexus. Spectra were acquired in the scan range 4000–530  $cm^{-1}$ , with a resolution of 4  $cm^{-1}$  (4 measurements were made for each material).  $^{13}C$  NMR were performed on spectrometer Bruker Avance 300 MHz. The tensile and elastic data were collected at room temperature with an Instron 4026. These parameters were measured per sample on ten replicates. The speed of the moving clamp was 100 mm/min. Received two types of mechanical hysteresis loops. The first type was obtained by stretching terpolymers at a constant elongation of 100%. Specimens were extended to 100% elongation and then they were allowed to relax and return to the initial gauge length. The cycle was repeated five times. Based on this measurement the per cent elastic recovery and permanent deformation of specimens were calculated. The second one was obtained by stretching a polymer sample from 10% to 100% at elongation growing by 10%. Before testing, all specimens were conditioned without any stress in a standard atmosphere ( $22 \pm 2$  °C,  $65 \pm 5\%$

humidity) for at least 24 hours. By the methods DSC (TA Instruments, heating-cooling-heating, 10 °C/min), DMTA (Rheovibron DDV-II, profiles for the examinations were made by injection molding) and WAXS (diffractometer Geiger-Flex, 2 $\theta$ : 5–38, 2 °C/min) the polymers' physical structure was evaluated.

## RESULTS AND DISCUSSION

To study the effect of macromolecule architecture on the properties of the materials obtained, a TPEEA series with a variable molar ratio of PTMO to PA12 block was synthesized. These terpolymers are composed of PTMO and PA12 blocks with a constant molecular weight of 1000 g/mol and 2000 g/mol, respectively, and the PTT block formed during synthesis. The type and molar and weight ratios of the substrates used for synthesis are shown in Table 1. Molar ratios characterize the architecture of terpolymer macromolecules (distribution of blocks) and weight ratios are related to the content of blocks.

The selected properties of TPEEA were presented in Table 2.

TPEEA with  $[\eta] > 1.25$  dL/g have molecular weights ensuring good mechanical properties<sup>23</sup>. All the materials obtained have  $[\eta]$  above this value. The water swelling results indicate the hydrophobic nature of all polymers obtained. The swelling does not exceed 2%, which indicates that water penetrates the amorphous phase of the polymer to a very small extent. Along with the increase in the content of ether blocks in the obtained copolymers, an increase in benzene absorption and a decrease in melting point and hardness is noticeable (Table 2). This proves that PTMO flexible blocks build the amorphous phase of the TPEEA and create more and better polymer matrix.

All obtained terpolymers have strength curves characteristic of elastomeric materials in which there is no yield point. Figure 1 shows only those samples that differ significantly in the course of the curves. Samples 1 and 2 (PTMO/PA12 = 2 and 2,5 respectively) have similar stress-elongation characteristics for polyesters and

**Table 1.** Compositions of the terpoly(ester-b-ether-b-amide)s

Sample No.	$M_{PA12}$ , g/mol	$M_{PTMO}$ , g/mol	$DP_{PTT}$	Molar ratio PTMO/PA12/DMT/1,3-PDO	$w_{PTMO}$	$w_{PA12}$	$w_{PTT}$	Expected structure of the terpolymer macromolecule
1	2000	1000	4	2/1/5/9	0.415	0.415	0.171	-( $ABCB$ ) <sub>n</sub> -
2	2000	1000	2.66	2,5/1/5/9	0.470	0.376	0.155	-
3	2000	1000	2	3/1/5/9	0.515	0.343	0.141	-[( $AB$ ) <sub>2</sub> $CB$ ] <sub>n</sub> -
4	2000	1000	1.6	3,5/1/5/9	0.553	0.316	0.130	-
5	2000	1000	1.33	4/1/5/9	0.586	0.293	0.121	-[ $(BA)_2BCB$ ] <sub>n</sub> -
6	2000	1000	1	5/1/5/9	0.639	0.256	0.105	-[ $(BA)_3BCB$ ] <sub>n</sub> -

M – molecular weight, DP – degree of polymerization, w – weight ratio, A – PTT, B – PTMO, C – PA12

**Table 2.** Properties of the TPEEA with varied molar ratio PTMO/PA12 and constant molecular weights of PA12=2000 g/mole and PTMO=1000 g/mole

Sample No.	$[\eta]$ , dL/g	MFI, g/10min	H, Shore A	H, Shore D	$p_{H_2O}$ , %	$p_b$ , %	$\sigma$ , MPa	E, MPa	$\epsilon$ , %	$T_m^i$ , °C	$T_m^e$ , °C
1	1,71	3,74	87,2	22,3	2	148	11,35	34,0	124	126	140
2	1,59	2,93	84,4	20,3	2	157	9,69	24,8	122	116	149
3	1,53	3,39	75,6	16,0	1	188	4,56	13,6	200	118	134
4	1,5	2,92	69,4	12,,3	2	190	2,96	13,3	201	112	123
5	1,33	2,41	65,2	11,3	2	197	3,06	9,88	201	110	120
6	1,27	2,45	49,4	<10	2	- <sup>c)</sup>	1,97	0,31	39	105	116

$[\eta]$  – limiting viscosity number, MFI – melt flow index, H – hardness,  $p_{H_2O}$  and  $p_b$  – absorbability of water and benzene, respectively,  $\sigma$  – tensile strength, E – the Young's modulus,  $\epsilon$  – elongation at break,  $T_m^i, T_m^e$  – initial and end of melting point

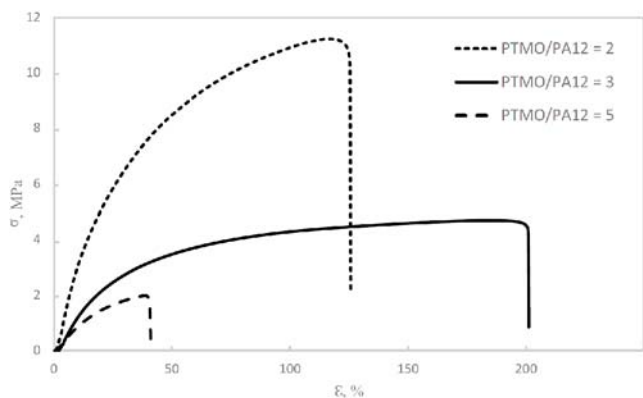


**Figure 1.** Strain-stress curves of terpolymers 1, 3 and 6

polyamides<sup>24-26</sup>. Materials 3, 4 and 5 (PTMO/PA12=3; 3,5 and 4) are typical elastomeric materials where the elongation exceeds 200%<sup>27, 28</sup>. The terpolymer with the highest content of flexible block (over 60%) has low mechanical strength, which is most likely due to the excessive dispersion of the hard domains in the large amorphous phase. To examine in detail the elastic properties of TPEEA, two types of mechanical hysteresis loops characterized by elasticity and stress relaxation in selected polymers were obtained (Figures 2 and 3).

The lowest values of permanent deformation after the first cycle of stretching (elastic returns after 100% elon-

gation reached 80%) showed terpolymers with a molar ratio of PTMO/PA12 blocks in the range from 3 to 4. In all samples between the first and second cycles, there were large energy losses due to the internal structuring of these copolymers. This behavior suggests that any products made of TPEEA must be pre-stretched before proper use. To better understand the nature of the deformations in the obtained terpolymers, the surface areas between the hysteresis curves and the x axis were calculated and assigned to individual accumulated or released energies during a single stretch-relaxation cycle (Table 3).

Sample No.	A	BII	BV	ΔB, %	C
1	195	131	62	53	441
2	166	100	47	53	351
3	115	63	25	61	138
4	87	43	20	53	138
5	81	40	14	64	87
6	–	–	–	–	–

A – field proportional to elastic dissipated energy, BII and BV – fields proportional to highly elastic dissipated energy during the second and fifth stretching cycle, ΔB – percentage change in the amount of highly elastic dissipated energy between the second and fifth cycles, C – field proportional to accumulated energy

**Table 3.** Surface areas proportional to accumulated and dispersed energy during TPEEA cyclic stretching

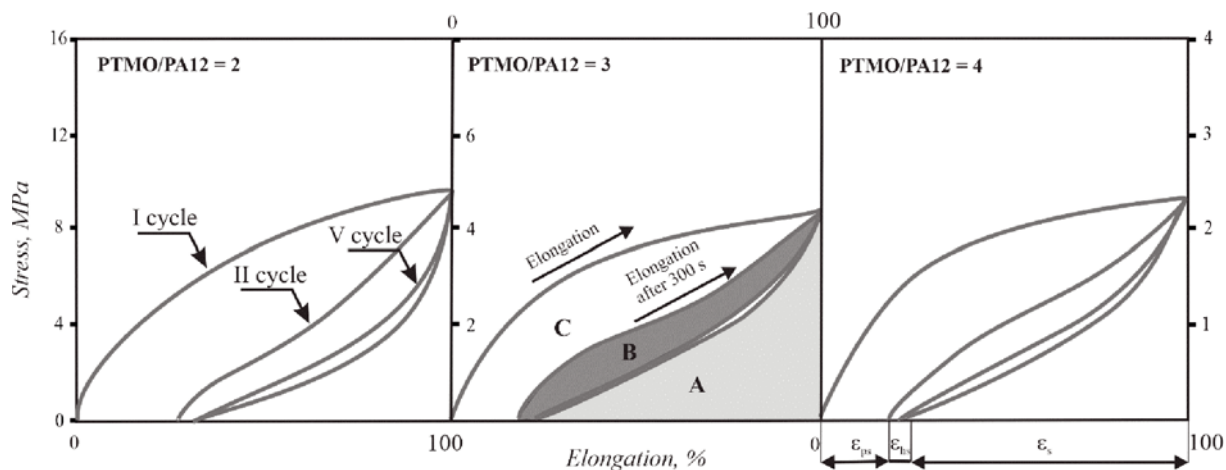


**Figure 2.** Mechanical hysteresis loops (5 cycles) at constant elongation by 100% of the terpolymers with varied molar ratio of ether and amide block and constant molecular weights of PA12 = 2000 g/mole and PTMO = 1000 g/mole. A – area proportional to elastic dissipated energy, B – area proportional to highly elastic dissipated energy, C – area proportional to accumulated energy,  $\epsilon_{ps}$  – irreversible elongation (permanent),  $\epsilon_{hs}$  – highly flexible elongation,  $\epsilon_s$  – elastic elongation

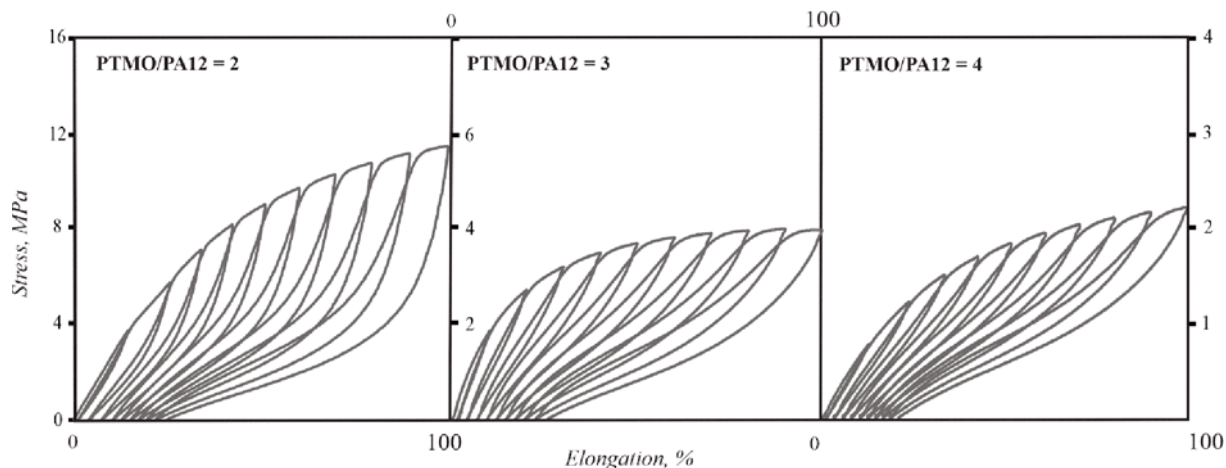


**Figure 3.** Mechanical hysteresis loops at elongation growing by 10% of the terpolymers with varied molar ratio of ether and amide block and constant molecular weights of PA12 = 2000 g/mole and PTMO = 1000 g/mole

The increase in the amount of PTMO flexible blocks improves the quality of the amorphous continuous phase, which results in a decrease in dispersed energy (responsible for both elastic and highly flexible response). Increasing the content of flexible blocks causes an increase in the volume of the polymer matrix and thus greater dispersion of the crystalline domains. As a result, they can more easily return to their pre-stretching state. This conclusion is confirmed by the decreasing values of energy accumulated in the first hysteresis cycle.

As the content of the ether block increased, the copolymers showed increasing strain values at break ( $\epsilon$ ) and decreasing values of breaking stress ( $\sigma$ ) and Young's modulus ( $E$ ).

The assumed chemical structure of synthesized terpolymers was confirmed by FT-IR (Fig. 4) and  $^{13}\text{C}$  NMR (Fig. 5) spectroscopy.

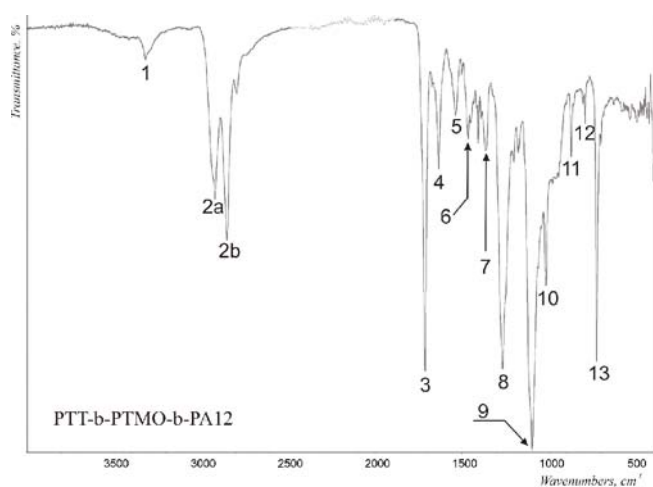


**Figure 4.** FT-IR spectrum of TPEEA with molar ratio of PTMO/PA12 = 3 and constant molecular weights of PA12 = 2000 g/mole and PTMO = 1000 g/mole (sample no. 3).

Analysis of FT-IR indicated the occurrence in the spectrograms of all characteristic bands for esters: symmetrical and asymmetrical stretching vibrations of the CH group in CH<sub>2</sub> groups (2), stretching vibrations of the carbonyl group C=O in ester bond (3), asymmetrical (8) and symmetrical (9) stretching vibrations (C-O-C) of ester segments, deformation vibrations of CH groups outside the plane bonds in the aromatic ring (13) and amides: stretching vibrations of NH groups bound by hydrogen bridges (1), I amide band (4), II amide band (5), III amide band (7), IV amide band (13) superimposed on the band corresponding to the vibrations of the CH groups in the aromatic ring.

Analysis of the  $^{13}\text{C}$  NMR spectra showed the presence of all characteristic groups present in the esters, ethers and amides. Signals are noted in the range 26.89–218.53 ppm. There are no signals derived from the carbon atoms of the carboxyl group. A 39.5 ppm chemical shift signal corresponds to an aliphatic-aliphatic ester group. Such binding can only be formed by reacting the carboxyl end groups of the oligoamide with an ester or ether block. Analyzing the above, it can therefore be concluded that the oligoamide was incorporated into the polymer macromolecule.

The effect of the PTMO/PA12 molar ratio on the thermal properties and physical structure of the copolymers were examined by WAXS (Fig. 6), DSC (Figs. 7, 8 and Table 4) and DMTA (Fig. 9) methods.

The diffraction pattern of the PA12 homopolymer has one broad diffraction maximum with two extreme points: 19.68° and 21.54°, which are the result of the overlap of reflections originating from two polymorphic structures  $\gamma$  and  $\alpha$  PA12. Terpolymer diffractograms have only reflections with the glancing angles  $2\Theta$  corresponding to the PA12 diffraction pattern values. There are no reflections typical of PTT. It can therefore be concluded that in the obtained multi-block copolymers made of rigid PTT and

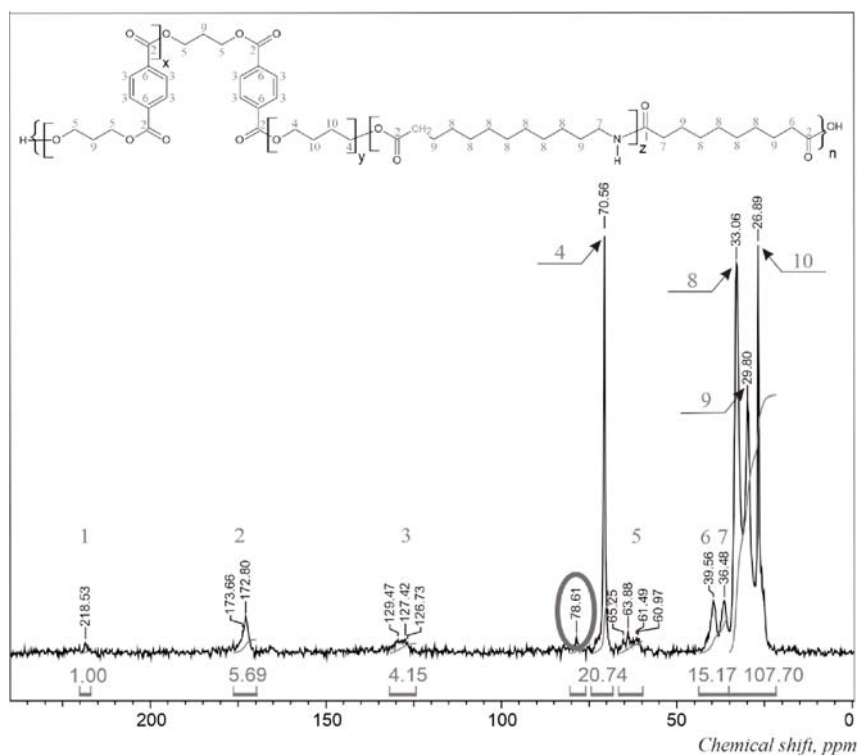


**Figure 5.**  $^{13}\text{C}$  NMR spectrum of TPEEA with molar ratio of PTMO/PA12 = 3 and constant molecular weights of PA12 = 2000 g/mole and PTMO = 1000 g/mole (sample no. 3)

**Table 4.** Selected thermal properties of the terpolymers produced

Sample No.	$T_{g1}$ , °C	$\Delta C_{p1}$ , J/g·°C	$T_{c1}$ , °C	$\Delta H_{c1}$ , J/g	$T_{m1}$ , °C	$\Delta H_{m1}$ , J/g	$T_{m2}$ , °C	$\Delta H_{m2}$ , J/g	$T_{g2}$ , °C	$\Delta C_{p2}$ , J/g·°C	$T_{c2}$ , °C	$\Delta H_{c2}$ , J/g	$T_{m3}$ , °C	$\Delta H_{m3}$ , J/g	$T_{m3}-T_{g1}$
1	-70	0.13	-	-	-4	1.46	56	3.22	45	0.072	67	16.80	109	9.10	179
2	-70	0.16	-	-	-5	3.32	44	2.60	40	0.041	60	13.10	107	8.86	177
3	-74	0.14	-	-	4	15.63	55	2.57	41	0.034	59	13.14	105	6.98	179
4	-73	0.14	-40	6.53	7	22.71	54	3.11	41	0.021	68	12.15	109	5.52	182
5	-72	0.16	-39	7.63	6	25.38	53	0.97	42	0.015	62	9.70	106	4.38	178
6	-72	0.17	-25	28.24	14	35.67	53	2.71	-	-	85	6.62	124	2.10	196

$T_{g1}$ ,  $T_{m1}$  – glass transition and melting point temperatures, respectively in low-temperature region;  $\Delta C_p$  – heat capacity change in  $T_{g1}$ ;  $\Delta H_{m1}$  – heat of melting at  $T_{m1}$ ;  $T_{m2}$ ,  $T_{m3}$ ,  $T_c$  – melting point temperatures and crystallization temperatures, respectively in high-temperature region,  $\Delta H_c$  – crystallization heat in  $T_c$ ;  $\Delta H_{m2}$  – heat of melting at  $T_{m2}$ ;  $\Delta H_{m3}$  – heat of melting at  $T_{m3}$ .

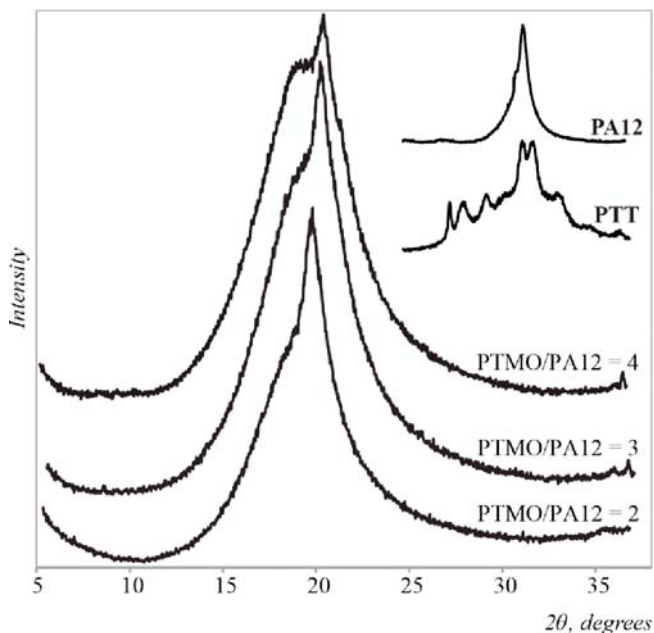


**Figure 6.** WAXS diffractograms of PA12 and selected terpolymers with varied molar ratio of ether and amide block and constant molecular weights of PA12 = 2000 g/mole and PTMO = 1000 g/mole

PA12 blocks, only the PA12 block is responsible for the formation of the crystalline phase.

Characteristic for the whole series is the constant value of the glass transition temperature of the low-temperature region (below room temperature) and the equal span of the glass transition temperature range. The glass transition temperature of PTMO homopolymer is  $-90$  °C. Chemical bonding of chain ends increases PTMO  $T_g$  by about 5–10 °C and the effect of the dispersed phase on this block by another 5 °C<sup>4</sup>. Therefore, the difference between PTMO glass

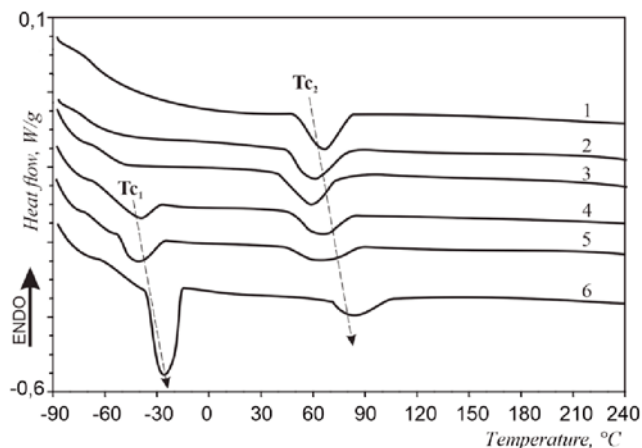


**Figure 8.** DSC cooling scans of the terpolymers TPEEA with varied molar ratio of ether and amide block and constant molecular weights of PA12 = 2000 g/mole and PTMO = 1000 g/mole

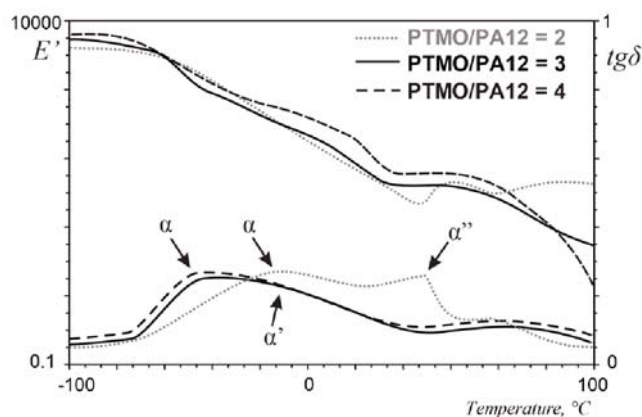


**Figure 9.** DMTA analysis of the terpolymers with varied molar ratio of ether and amide block and constant molecular weights of PA12 = 2000 g/mole and PTMO = 1000 g/mole

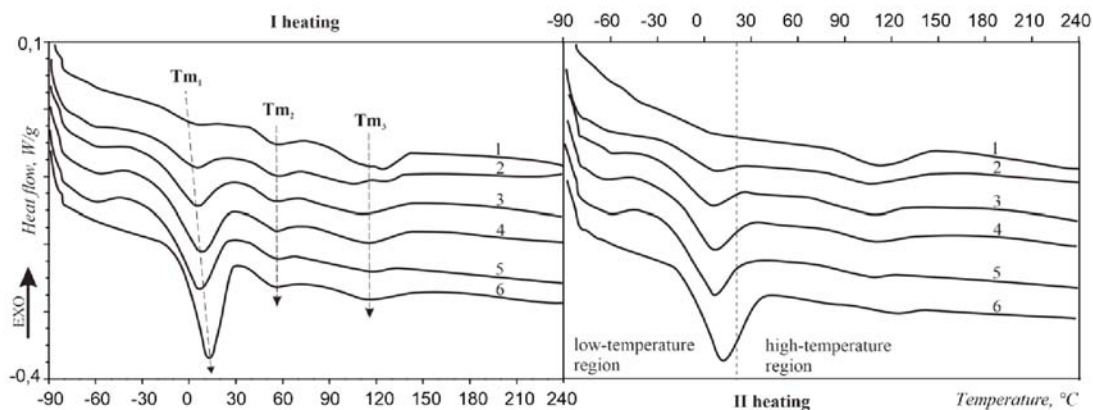


**Figure 7.** DSC first and second heating scans of the terpolymers TPEEA with varied molar ratio of ether and amide block and constant molecular weights of PA12 = 2000 g/mole and PTMO = 1000 g/mole

transition temperatures and terpolymers obtained up to 20 °C cannot be explained only by stiffening of the chain ends and interfacial interactions. The dissolution of short, non-crystallizing ester sequences in the PTMO block phase is probably responsible for further  $T_{g1}$  increase in terpolymers. According to the R. L. Scott solubility criterion, it is possible to obtain a real PTT/PTMO solution when the degree of polymerization of the PTT block is less than 2.  $T_{g2}$  is the glass transition temperature of the PA12 amorphous phase containing PTT sequences. A pure PA12 block has a  $T_g = 45$  °C and PTT  $T_g = 55$  °C. For the mixture of these blocks, the well-known phenomenon of  $T_g$  depression is observed. As the PTMO/PA12 molar ratio increases, the temperature and melting heat of the crystalline fraction of PTMO blocks increases and the melting endotherms become slender. This demonstrates the improving phase separation of the soft phase. As the content of flexible blocks increases, the melting enthalpy and the melting point ( $T_{m1}$ ) of the PTMO blocks increase. Most likely, an increasingly better-formed polymer matrix is being formed.

There are two melting endotherms in the high temperature area. The thermal effect at a temperature of about 50 °C ( $T_{m2}$ ) is characteristic for many melt crystallizing polymers and is responsible for the melting of para-crystalline and microcrystalline formations and defective structures. The second endotherm ( $T_{m3}$ ) determines the temperature and heat of fusion of the terpolymer crystalline phase. Endotherms determining the temperature and heat of fusion are very flattened and reach maxima on average around 100 °C. All melting endotherms in the high temperature area are very wide, which indicates the heterogeneity of the crystalline phase. In addition, they are characterized by a significant decrease in melting point compared to PA12 homopolymer. This indicates that in the synthesized terpolymers the crystalline phase is essentially in decline and is very defective. Confirmation of this application can be found in the cooling cycle. Cooling DSC curves have broad exotherms of PA12 blocks and increasingly well-developed PTMO exotherms.

Figure 9 shows the effect of temperature on the dynamic, mechanical properties of TPEEA depending on the PTMO/PA12 molar ratio. The temperature spectra obtained are characteristic curves for thermoplastic elastomers. The spectra of the storage modulus have three temperature regions: range from -110 °C to -70 °C (value of the storage modulus above 1 GPa characteristic for the glassy state), range from -70 °C to 15 °C (viscoelastic relaxation processes), range from 15 °C to 70 °C (highly elastic state observed in the form of "Plateau of flexibility"). All  $tg\delta$  maxima are the superposition of at least two relaxation transitions associated with the glassy transitions of PTMO ( $\alpha$ ) and interphase ( $\alpha'$ ) (a mixture of blocks occurring at the phase boundary resulting from covalent bonds between blocks). As the PTMO/PA12 molar ratio increases, the  $tg\delta$  maxima shift towards lower temperatures. Maximum  $\alpha''$  is a relaxation transition associated with the amorphous phase of PA12.

## CONCLUSIONS

Synthesis parameters (temperature, time, pressure, catalyst concentration) of a new type of terpoly(ester-b-ether-b-amides) with a variable molar ratio of ether to amide block were selected. The copolymer microstructure was assessed based on DSC, DMTA and WAXS analyses. The synthesized copolymers were found to be typical elastothermoplasts and have a multi-phase (crystalline-amorphous) physical structure. The amorphous phases (matrix) are made of PTMO flexible blocks contaminated with short ester sequences ( $T_{g1}$ ) and a mixture of ester and amide blocks ( $T_{g2}$ ). The crystal phase (domains) is made of PA12 rigid blocks and is disturbed by inclusions of PTT blocks. With the increasing molar ratio of ether to amide block in TPEEA, the proportion of soft phase increases, while the content of hard phase and interphase decreases. The synthesized multi-block copolymers were characterized by good mechanical properties, including good flexibility, thermostability, and thermal and chemical resistance. TPEEA can successfully meet the specific requirements of many industries.

## LITERATURE CITED

1. Aleksandrovic, V., Djonlagic, J. (2001). Synthesis and characterization of thermoplastic copolyester elastomers modified with fumaric moieties. *J. Serb. Chem. Soc.* 66(3), 139–152. DOI: 10.2298/JSC0103139A.
2. Van der Schuur, M., Gaymans, R. (2007). Influence of morphology on the properties of segmented block copolymers. *Polymer*, 48, 1998–2006. DOI: 10.1016/j.polymer.2007.01.063.
3. Wilson, R., Divakaran, A., Kiran, S., Varyambath, A., Kumaran, A., Sivaram, S., Ragupathy, L. (2018). Poly(glycerol sebacate)-Based Polyester–Polyether Copolymers and Their Semi-Interpenetrated Networks with Thermoplastic Poly(ester-ether) Elastomers: Preparation and Properties. *ACS Omega*. 3, 18714–18723. DOI: 10.1021/acsomega.8b02451.
4. Holden, G. (2011). Thermoplastic Elastomers. In M. Kutz (Ed.), *Appl. Plastics Engin. Handbook*, 77–91, Waltham, Elsevier.
5. Holden, G., Bishop, E., Legge, N. (1969). Thermoplastic elastomers. *J. Polym. Sci.* 26, 1, 37–57. DOI: 10.1002/polc.5070260104.
6. Balta Calleja F.J., Roslaniec, Z. (2000). *Block copolymers*, New York, Marcel Dekker.
7. Zhang, J., Deubler, R., Hartlieb, M., et al. (2017). Evolution of Microphase Separation with Variations of Segments of Sequence-Controlled Multiblock Copolymers. *Macromolecules*, 50, 18, 7380–7387. DOI: 10.1021/acs.macromol.7b01831.
8. Bates, F.S., Fredrickson, G.H. (1999). Block Copolymers—Designer Soft Materials. *Physics Today*, 52, 33–38. DOI: 10.1063/1.882522.
9. Armstrong, S., Freeman, B., Hiltner, A., Baer, E. (2012). Gas permeability of melt-processed poly(ether block amide) copolymers and the effects of orientation. *Polymer*. 53, 1383–1392. DOI: 10.1016/j.polymer.2012.01.037.
10. Krijgsman, J., Husken, D., Gaymans, R. (2003). Synthesis and properties of thermoplastic elastomers based on PTMO and tetra-amide. *Polymer*, 44, 7573–7588. DOI: 10.1016/j.polymer.2003.09.043.
11. Yang, I., Tsai, P. (2006). Intercalation and viscoelasticity of poly(ether-block-amide) copolymer/montmorillonite nanocomposites: Effect of surfactant. *Polymer*, 47, 5131–5140. DOI: 10.1016/j.polymer.2006.04.065.
12. Nojima, S., Kiji, T., Ohguma, Y. (2007). Characteristic Melting Behavior of Double Crystalline Poly( $\epsilon$ -caprolactone)-block-polyethylene Copolymers. *Macromolecules*, 40, 21, 7566–7572. DOI: 10.1021/ma0627830.

13. Klinedinst, D., Yilgör, I., Yilgör, E., et al. (2012). The effect of varying soft and hard segment length on the structure–property relationships of segmented polyurethanes based on a linear symmetric diisocyanate, 1,4-butanediol and PTMO soft segments. *Polymer*, 53, 5358–5366. DOI: 10.1016/j.polymer.2012.08.005.
14. Winnacker, M., Rirger, B. (2015). Poly(ester amide)s: recent insights into synthesis, stability and biomedical applications. *Polym. Chem.* 7, 7039–7046. DOI: 10.1039/C6PY01783E.
15. Rodriguez-Galan, A., Lourdes, F., Puiggali, J. (2010). Degradable Poly(ester amide)s for Biomedical Applications. *Polymers*, 3(1), 1634–1645. DOI: 10.3390/polym3010065.
16. Sijbrandi, N., Kimenai, A., Mes E., et al. (2012). Synthesis, Morphology, and Properties of Segmented Poly(ether amide)s with Uniform Oxalamide-Based Hard Segments. *Macromolecules*, 45, 9, 3948–3961. DOI: 10.1021/ma2022309.
17. Fu, T., Wei, Y., Cheng, P., et al. (2018). A Novel Biodegradable and Thermosensitive Poly(Ester-Amide) Hydrogel for Cartilage Tissue Engineering. *BioMed Research International*. Art. id 2710892. Retrieved June 2, 2021 from Hindawi.com database on the World Wide Web: <https://www.hindawi.com>. DOI: 10.1155/2018/2710892.
18. Zeng, F., Xu, J., Sun, L., et al. (2020). Copolymers of  $\epsilon$ -caprolactone and  $\epsilon$ -caprolactam via polyesterification: towards sequence-controlled poly(ester amide)s. *Polym. Chem.* 11, 1211–1219. DOI: 10.1039/C9PY01388A.
19. Goonoo, N., Bhaw-Luximon, A., Bowlin, G., Jhurry, D. (2012). Diblock Poly(ester)-Poly(ester-ether) Copolymers: I. Synthesis, Thermal Properties, and Degradation Kinetics. *Ind. Eng. Chem. Res.* 51, 37, 12031–12040. DOI: 10.1021/ie301703j.
20. Xu, Q., Tang, L., Wang, Ch., et al. (2017). Effects of Poly(Ethylene Glycol) Segment on Physical and Chemical Properties of Poly(Ether Ester) Elastomers. *Materials Science Forum*, 898, 2147–2157. Retrieved June 10, 2021 from Scientific.net database on the World Wide Web: <https://www.scientific.net>. DOI: 10.4028/www.scientific.net/MSF.898.2147.
21. Catiker, E., Ozturk, T., Atakay, M., et al. (2019). Synthesis and characterization of novel ABA type poly(Ester-ether) triblock copolymers. *J. Polym. Res.* 26, 123–126. DOI: 10.1007/s10965-019-1778-5.
22. Peng, X., Behl, M., Zhang, P., et al., (2017). Synthesis and Characterization of Multiblock Poly(Ester-Amide-Urethane)s. *MRS Advances*, 2, 2551–2559. DOI: 10.1557/adv.2017.486.
23. Van Krevelen, D.W., Te Nijehuis, K. (2009). *Properties of Polymers*, Amsterdam, Elsevier.
24. Scheirs, J., Long, T.E. (2003). *Modern Polyesters: chemistry and technology of polyesters and copolyesters*, Hoboken, John Wiley & Sons.
25. Touris, A., Turcios, A., Mintz, E., et al. (2020). Effect of molecular weight and hydration on the tensile properties of polyamide 12. *Results in Materials*, 8, 100149. DOI 10.1016/j.rinma.2020.100149.
26. O'Connor, H.J., Dickson, A.N., Dowling, D.P. (2018). Evaluation of the mechanical performance of polymer parts fabricated using a production scale multi jet fusion printing process. *Additive Manufacturing*, 22, 381–387. DOI: 10.1016/j.addma.2018.05.035
27. Rosenbloom, S.I., Gentekos, D.T., Silberstein, M.N., Fors, B.P. (2020). Tailor-made thermoplastic elastomers: customisable materials via modulation of molecular weight distributions. *Chem. Sci.* 11, 1361–1367. DOI: 10.1039/C9SC05278J.
28. Cho, H., Mayer, S., Poselt, E., et al. (2017). Deformation mechanisms of thermoplastic elastomers: Stress-strain behavior and constitutive modeling. *Polymer*, 128, 87–99. DOI: 10.1016/j.polymer.2017.08.065.